Supporting Information for:

Synthesis, Crystal Structure and Physical Properties of the Type-I Clathrate

$Ba_{8-\delta}Ni_x\square_y Si_{46-x-y}$
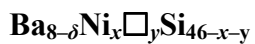
U. Aydemir*, C. Candolfi, A. Ormeci, H. Borrmann, U. Burkhardt, Y. Oztan, N. Oeschler, M. Baitinger, F. Steglich and Yu. Grin*

Max-Planck-Institut für Chemische Physik fester Stoffe, Dresden, Germany

* To whom correspondence should be addressed. E-mail: aydemir@cpfs.mpg.de, grin@cpfs.mpg.de. Tel.: +49-351-46464000.

S1. X-ray Absorption Spectroscopy Measurements. Around 20 mg of samples were ground into fine powders and mixed with B_4C and paraffin wax. Samples were then placed on Kapton foils with an area of 1 cm^2. Wavelength selection was realized by means of Si (111) double crystal monochromator. The energy range 8150 eV $< E <$ 9600 eV was scanned with an EXAFS program starting with constant energy step size $\Delta E =$ 0.2 eV / (integration time $t = 1$ sec) in the XANES region close to the Ni K-edge and a constant step size in reciprocal space with $\Delta k = \sqrt{(E-E_{Ni})} = 7 \times 10^{-3}\text{Å}^{-1}$ in the EXAFS region. In total, 660 points and an increasing integration time up to 5 sec at 9600 eV led to 30 min per scan. The absorption $\mu(E) = -\ln(I_1/I_0)$ was calculated from the measured intensities at ionization chambers C_1 and C_0 which were arranged behind and in front of the sample. For spectra evaluations, two successively measured spectra were averaged. The energy values were calibrated by means of the first inflection point of the simultaneously measured reference spectrum of Ni foil ($E_{Ni} = 8333$ eV). EXAFS data analyses were carried out using IFEFFIT program package.[1-3] Normalization of the absorption spectra $\mu(E)$ and the extraction of the EXAFS interference function $\chi(k)$ was performed with a standard procedure including pre- and post-edge background removal. The applied cut-off value of $R = 1.17$ Å corresponds roughly to half of the shortest distances (Ni – Si ≈ 2.3 Å) in the crystal structure of the clathrate phase. To enhance the features at higher k values, the EXAFS oscillations were multiplied by a scaling factor k^2.

1.   Newville, M., *J. Synchrotron Radiat.* **2001,** *8*, 96-100.
2.   Newville, M., *J. Synchrotron Radiat.* **2001,** *8*, 322-324.
3.   Ravel, B.; Newville, M., *J. Synchrotron Radiat.* **2005,** *12*, 537-541.
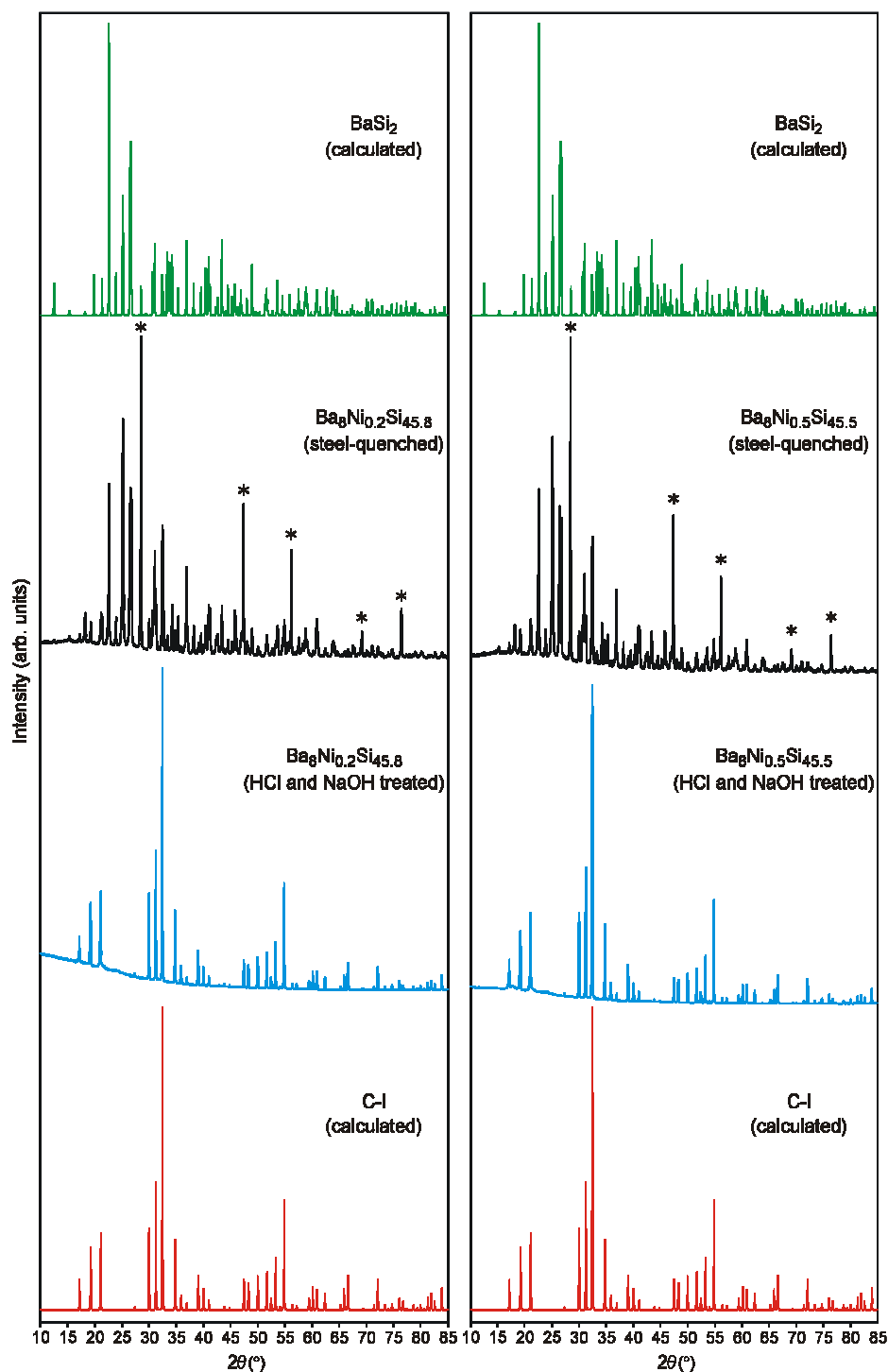
Figure S1: PXRD patterns (Cu-$K\alpha_1$ radiation) of the samples with nominal compositions $Ba_8Ni_{0.2}Si_{45.8}$ (left) and $Ba_8Ni_{0.5}Si_{45.5}$ (right) after steel-quenching (black) and after treatment with dilute HCl and NaOH (blue). Theoretical patterns of clathrate-I ($Ba_8Ni_{3.7}Si_{41.4}\square_{0.9}$) and $BaSi_2$ are shown for comparison; α-Si reflections are indicated with asterisks. After treatment with HCl and then with NaOH, single phase clathrates were obtained.
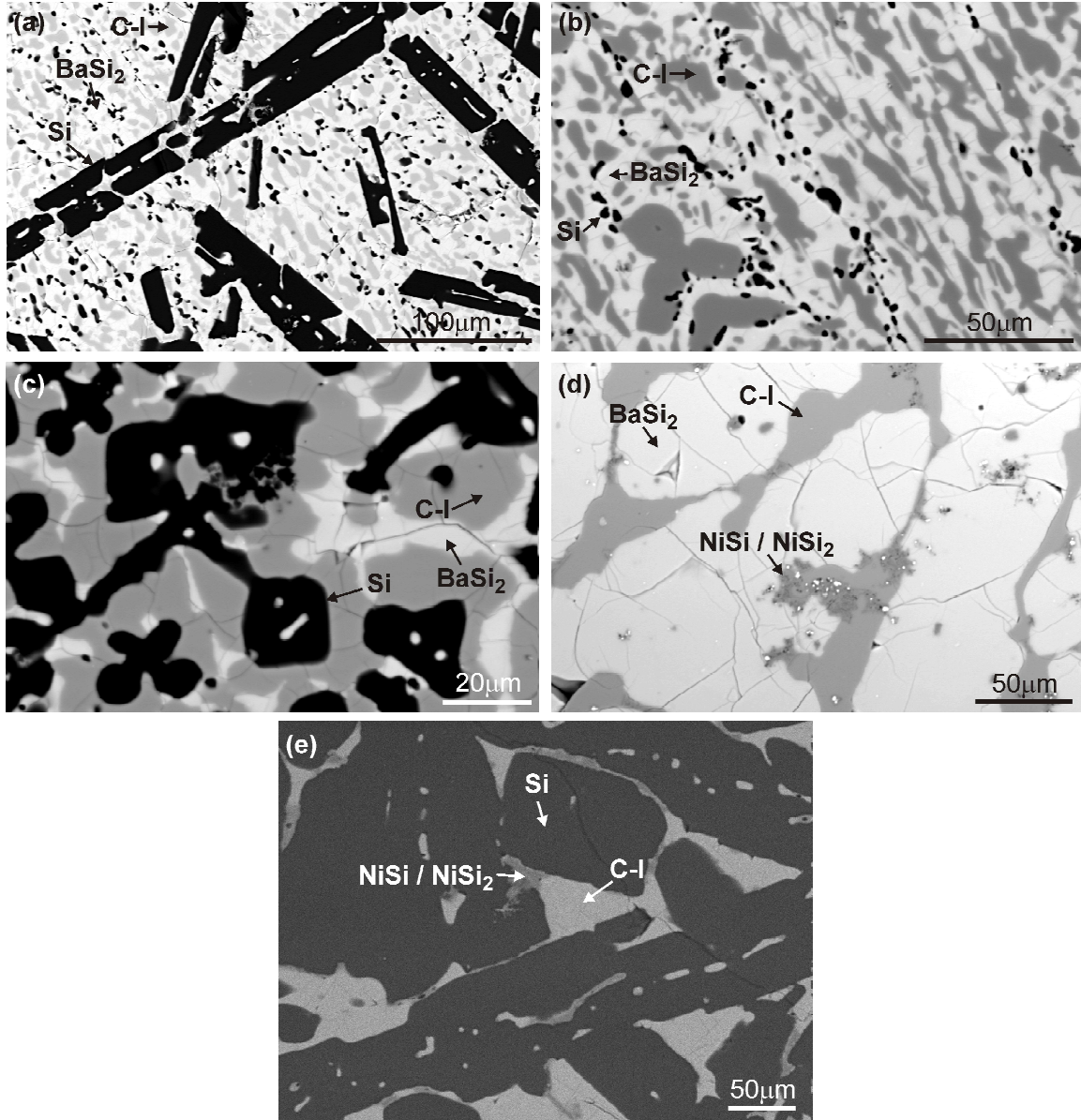
Figure S2: Microstructure (SEM, BSE contrast) of the samples with nominal compositions (**a**) $Ba_8Ni_{0.5}Si_{45.5}$ (sample 1), (**b**) $Ba_{22.5}Ni_{2.5}Si_{75}$ (sample 3), (**c**) $Ba_{10}Ni_2Si_{88}$ (sample 4), (**d**) $Ba_{25}Ni_5Si_{70}$ (sample 7), and (**e**) $Ba_{2.5}Ni_{2.5}Si_{95}$ (sample 8) obtained after annealing at 1000 °C. Sample numbers are given according to Fig. 1 and observed phases are marked with arrows.
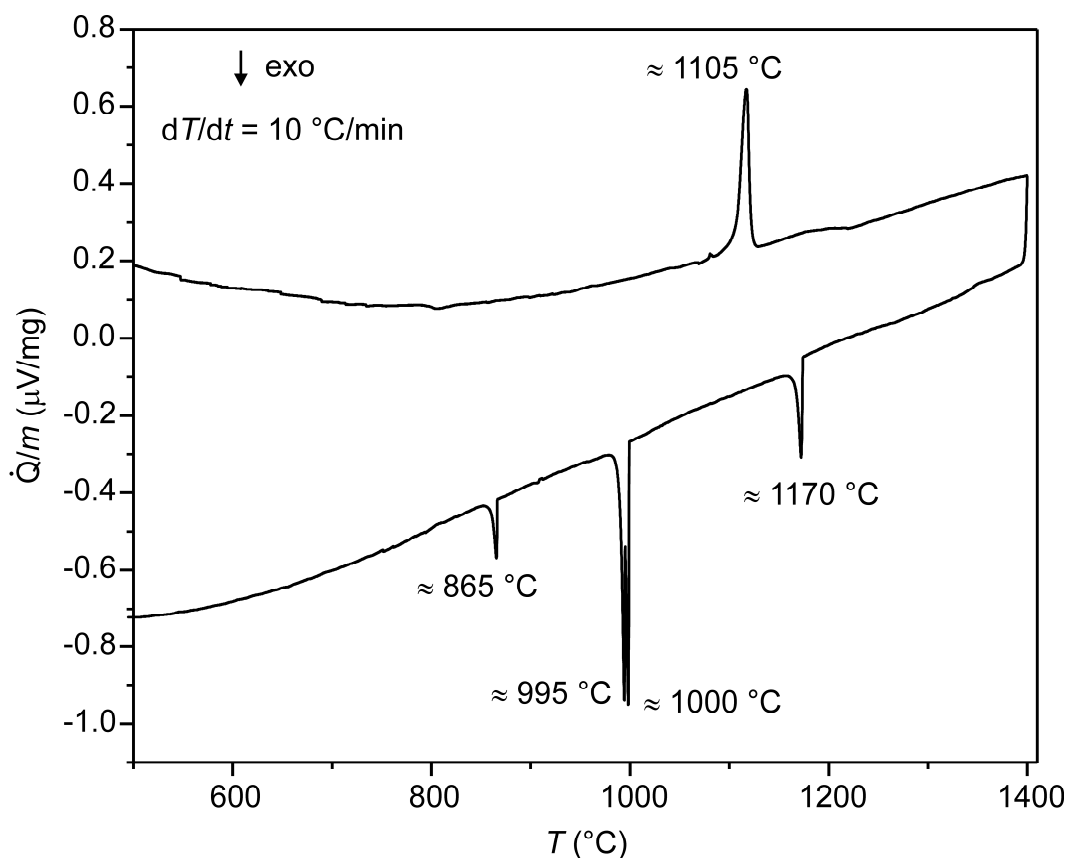
Figure S3: Heat-flux DSC measurement of the sample $Ba_8Ni_{3.5}Si_{42.5}$ prepared by annealing at 1000 °C. The peritectic temperature at this composition was estimated to be 1105 °C from the heating curve. This temperature was found to be almost invariant for the clathrate samples with other compositions. Complete melting of the sample is indicated by the broad endothermic effect following the peritectic reaction. In agreement with the microstructure analysis, the exothermic peak on cooling at 1170 °C corresponds to the primary crystallization of α-Si, and the peak at 1000 °C to the crystallization of the clathrate phase. The peaks at 995 °C and 865 °C may indicate a cotectic formation of $BaSi_2$ and clathrate-I phase and ternary eutectic, respectively.

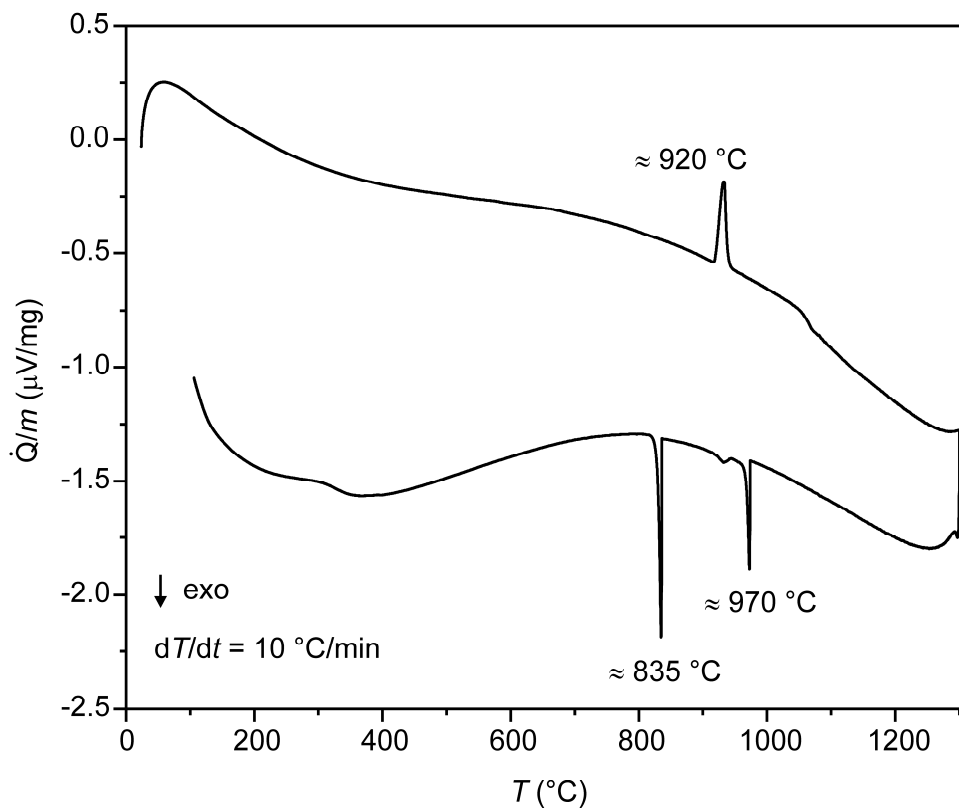**Figure S4:** Thermal behavior of the sample with the nominal composition $BaNiSi_3$ melting at the eutectic temperature (920 °C, onset) of the quasi-binary system $BaSi_2$ - NiSi. The peaks on cooling at around 970 °C may correspond to the primary formation of $BaSi_2$ or the cotectic formation of $BaSi_2$ and NiSi. The peak at 835 °C may indicate the eutectic crystallization.
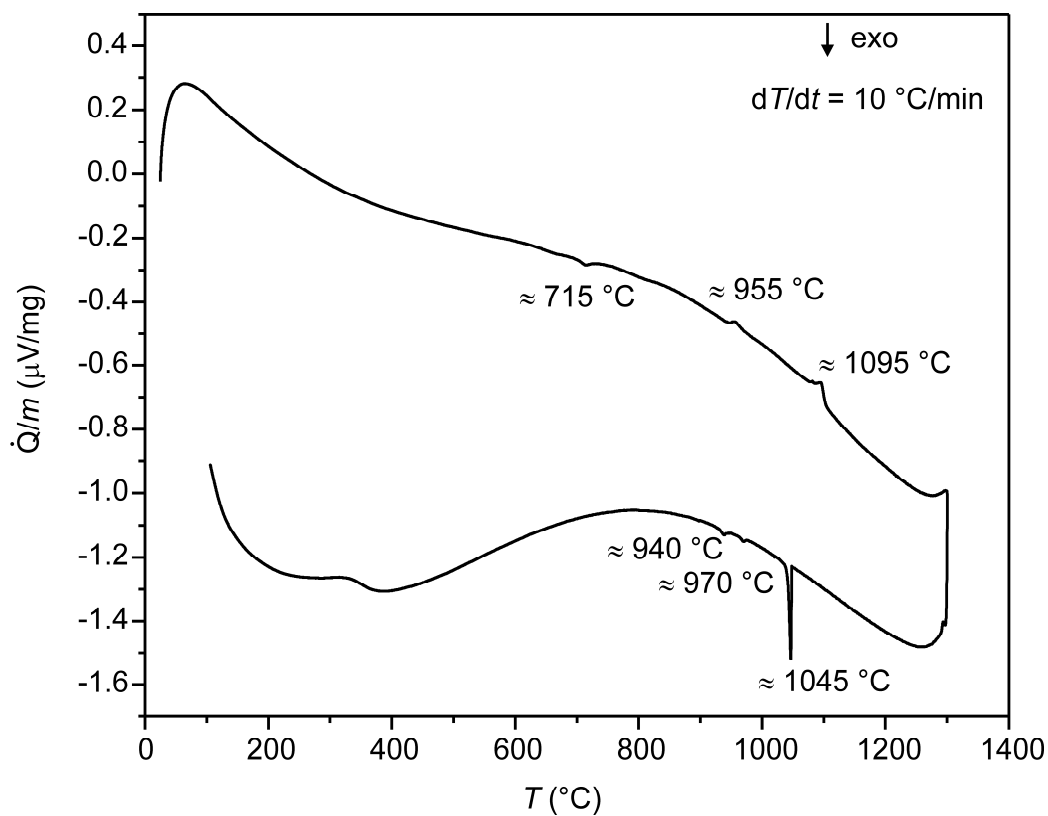
Figure S5: Heat-flux DSC measurement of the clathrate $Ba_{7.9(1)}Ni_{1.6(1)}Si_{44.4(1)}$ obtained after steel-quenching. The exothermic effect at around 715 °C on heating indicates that the clathrate phase is metastable at this composition. The endothermic effect at around 1095 °C on heating is in agreement with the observed peritectic reaction temperatures of the annealed clathrate-I samples. The main exothermic peak at 1045 °C on cooling may indicate the crystallization of the clathrate-I phase or α-Si from the melt.
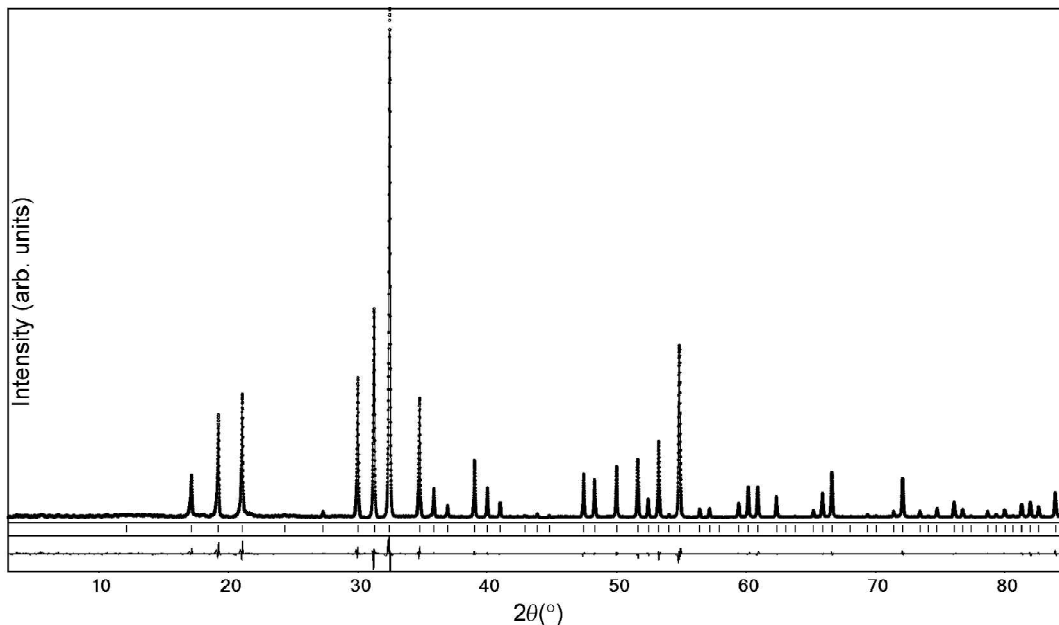
Figure S6: PXRD pattern (Cu-$K\alpha_1$ radiation) of the sample with composition $Ba_{7.9(1)}Ni_{1.4(1)}Si_{44.6(1)}$ (dotted line). The calculated profile after Rietveld refinement (solid line) and difference curve (below) are shown. The ticks mark the calculated reflection positions of the clathrate-I phase.

Figure S7: PXRD pattern (Cu-$K\alpha_1$ radiation) of the sample with composition $Ba_{7.9(1)}Ni_{1.6(1)}Si_{44.4(1)}$ (dotted line). The calculated profile after Rietveld refinement (solid line) and difference curve (below) are shown. The ticks mark the calculated reflection positions of the clathrate-I phase.
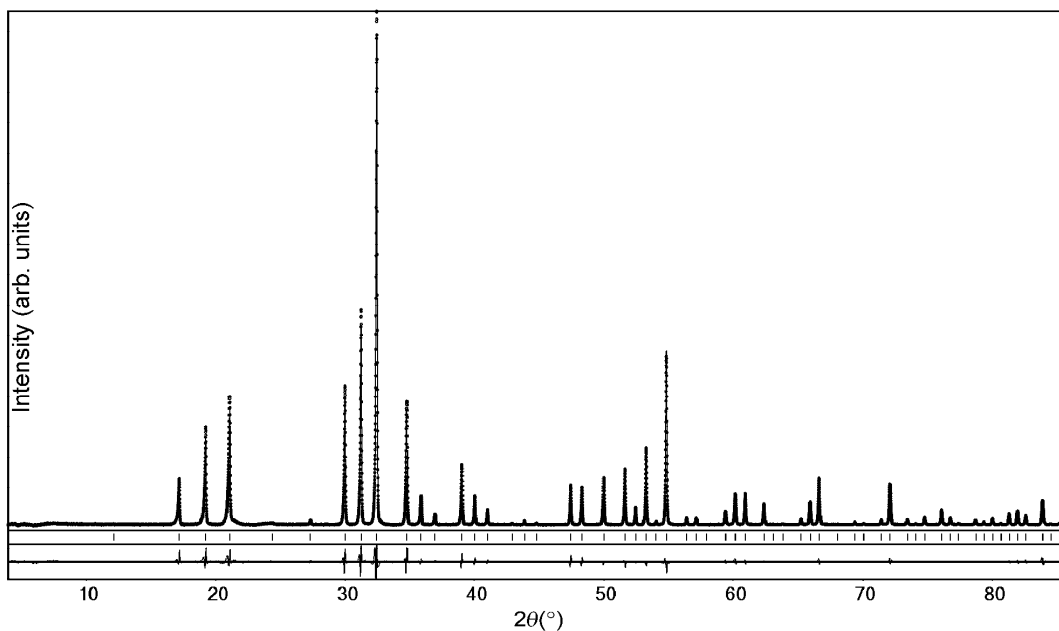
Table S1: Interatomic distances with multiplicity *n* for the single crystal of $Ba_8Ni_{2.6}Si_{43.3}\square_{0.1}$. The sites Si31 and Si32 represent alternatively occupied positions of the site Si3.

Atoms		*n*	*d* / Å	Atoms		*n*	*d* / Å
Ba1	– Si2	8 ×	3.2929(6)	Ni1	– Si32	4 ×	2.284(2)
	– Si31	12 ×	3.399(2)	Si1	– Si31	4 ×	2.402(2)
	– Si32	12 ×	3.500(2)				
Ba2	– Si31	2 ×	3.343(6)	Si2	– Si2	1 ×	2.3327(8)
	– Si32	2 ×	3.354(6)		– Si31	3 ×	2.396(1)
	– Si31	2 ×	3.421(6)		– Si32	3 ×	2.399(2)
	– Si32	2 ×	3.423(6)				
	– Si31	2 ×	3.536(6)	Si31	– Si2	2 ×	2.396(1)
	– Si31	2 ×	3.537(6)		– Si31	1 ×	2.398(2)
	– Si32	2 ×	3.541(6)		– Si1	1 ×	2.402(2)
	– Ni1/Si1	1 ×	3.543(6)		– Si32	1 ×	2.517(3)
	– Si32	2 ×	3.551(6)				
	– Ni1/Si1	2 ×	3.627(6)	Si32	– Ni1	1 ×	2.284(2)
	– Si2	2 ×	3.676(3)		– Si2	2 ×	2.399(2)
	– Si32	1 ×	3.728(4)		– Si31	1 ×	2.517(3)
	– Si2	2 ×	3.747(2)		– Si32	1 ×	2.635(3)
	– Ni1/Si1	1 ×	3.780(6)				
	– Si31	1 ×	3.834(4)				
	– Si32	2 ×	3.889(3)				
	– Si2	2 ×	3.914(2)				
	– Si2	2 ×	3.963(3)				
	– Si31	2 ×	3.996(2)				
	– Si32	1 ×	4.060(4)				
	– Si31	1 ×	4.167(4)				

Table S2: Interatomic distances with multiplicity *n* for the single crystal of $Ba_8Ni_{3.2}Si_{42.4}\square_{0.4}$. The sites Si31, Si32 and Si33 represent alternatively occupied positions of the site Si3.

Atoms		n	d / Å	Atoms		n	d / Å
Ba1	– Si2	8 ×	3.2862(6)	$\square$	– Si33	4 ×	2.146(13)
	– Si31	12 ×	3.361(2)	Ni1	– Si32	4 ×	2.279(2)
	– Si32	12 ×	3.502(2)	Si1	– Si31	4 ×	2.443(2)
	– Si33	12 ×	3.639(13)				
Ba2	– Si33	2 ×	3.264(9)	Si2	– Si2	1 ×	2.3409(8)
	– Si31	2 ×	3.298(2)		– Si31	3 ×	2.395(1)
	– Si32	2 ×	3.312(1)		– Si32	3 ×	2.397(1)
	– Si33	2 ×	3.421(9)		– Si33	3 ×	2.463(8)
	– Si33	2 ×	3.424(8)				
	– Si31	2 ×	3.473(2)	Si31	– Si31	1 ×	2.311(3)
	– Si31	2 ×	3.475(1)		– Si2	2 ×	2.395(1)
	– Si32	2 ×	3.477(1)		– Si1	1 ×	2.443(2)
	– Si32	2 ×	3.479(1)		– Si32	1 ×	2.476(2)
	– Si33	2 ×	3,540(9)		– Si33	1 ×	2.528(13)
	– Si31	2 ×	3.572(1)				
	– Ni1/Si1	2 ×	3,5774(5)	Si32	– Ni1	1 ×	2.279(2)
	– Si32	2 ×	3.588(1)		– Si2	2 ×	2.397(1)
	– Ni1/Si1	1 ×	3.6031(8)		– Si31	1 ×	2.476(2)
	– Si2	2 ×	3.68151(9)		– Si32	1 ×	2.638(2)
	– Si33	1 ×	3.742(13)		– Si33	1 ×	2.685(13)
	– Si32	1 ×	3.757(2)				
	– Si2	2 ×	3.7687(7)	Si33	– $\square$	1 ×	2.146(13)
	– Ni1/Si1	1 ×	3.8091(8)		– Si2	2 ×	2.463(8)
	– Si33	2 ×	3.851(13)		– Si31	1 ×	2.528(13)
	– Si32	2 ×	3.874(2)		– Si32	1 ×	2.685(13)
	– Si31	1 ×	3.901(2)		– Si33	1 ×	2.73(2)
	– Si2	2 ×	3.9152(7)				
	– Si2	2 ×	3.9346(9)				
	– Si31	2 ×	4.024(2)				
	– Si33	1 ×	4.031(13)				
	– Si32	1 ×	4.048(2)				
	– Si31	1 ×	4.194(2)				

Table S3: Interatomic distances with multiplicity n for the single crystal of $Ba_8Ni_{3.7}Si_{41.4}\square_{0.9}$. The sites Si31, Si32 and Si33 represent alternatively occupied positions of the site Si3.

Atoms		n	d / Å	Atoms		n	d / Å
Ba1	– Si2	8 ×	3.2857(5)	□	– Si33	4 ×	2.188(5)
	– Si31	12 ×	3.356(3)	Ni1	– Si32	4 ×	2.332(1)
	– Si32	12 ×	3.454(1)	Si1	– Si31	4 ×	2.455(3)
	– Si33	12 ×	3.587(5)				
Ba2	– Si31	2 ×	3.318(2)	Si2	– Si2	1 ×	2.3405(7)
	– Si33	2 ×	3.334(3)		– Si32	3 ×	2.3935(9)
	– Si32	2 ×	3.339(1)		– Si31	3 ×	2.406(2)
	– Si31	2 ×	3.455(2)		– Si33	3 ×	2.420(3)
	– Si31	2 ×	3.457(2)				
	– Si33	2 ×	3.457(3)	Si31	– Si31	1 ×	2.253(4)
	– Si33	2 ×	3.463(3)		– Si32	1 ×	2.394(3)
	– Si32	2 ×	3.470(1)		– Si2	2 ×	2.406(2)
	– Si33	2 ×	3,474(1)		– Si1	1 ×	2.455(3)
	– Si31	2 ×	3.532(2)		– Si33	1 ×	2.513(6)
	– Si33	2 ×	3,551(3)				
	– Si32	2 ×	3.555(1)	Si32	– Ni1	1 ×	2.332(1)
	– Ni1/Si1	2 ×	3.5905(7)		– Si2	2 ×	2.3935(9)
	– Ni1/Si1	1 ×	3.607(1)		– Si31	1 ×	2.394(3)
	– Si2	2 ×	3.709(1)		– Si32	1 ×	2.534(2)
	– Si33	1 ×	3.732(5)		– Si33	1 ×	2.651(5)
	– Ni1/Si1	1 ×	3.773(1)				
	– Si2	2 ×	3.7776(7)	Si33	– □	1 ×	2.188(5)
	– Si33	2 ×	3.823(5)		– Si2	2 ×	2.420(3)
	– Si32	1 ×	3.826(2)		– Si31	1 ×	2.513(6)
	– Si2	2 ×	3.8952(7)		– Si32	1 ×	2.651(5)
	– Si2	2 ×	3.912(1)		– Si33	1 ×	2.765(7)
	– Si32	2 ×	3.922(1)				
	– Si31	1 ×	3.955(3)				
	– Si33	1 ×	3.965(5)				
	– Si31	2 ×	4.054(3)				
	– Si32	1 ×	4.060(2)				
	– Si31	1 ×	4.190(3)				

Table S4: Crystallographic data for the steel-quenched clathrate samples.

Refined composition	$Ba_{7.88(2)}Ni_{1.39(3)}Si_{44.61(3)}$	$Ba_{7.90(2)}Ni_{1.60(4)}Si_{44.40(4)}$
EDXS composition	$Ba_{7.5}Ni_{1.6}Si_{44.4}$	$Ba_{7.5}Ni_{1.8}Si_{44.2}$
Space group; Z	$Pm\bar{3}n$ (no. 223); 1	
a (Å)	10.3088(1)	10.3078(1)
Diffractometer	Guinier - Huber G670 camera	
Radiation; λ (Å)	Cu-$K\alpha_1$; 1.54056	
Measured range (°); 2θ step (°)	$5 \leq 2\theta \leq 85$; $\Delta 2\theta = 0.005$	
R_i; R_p	0.027; 0.084	0.026; 0.109

Table S5: Atomic coordinates, displacement parameters (in Å^2) and site occupancies for $Ba_{7.88(2)}Ni_{1.39(3)}Si_{44.61(3)}$.

Atom	Site	x	y	z	U_{eq}	Occ.
Ba1	2a	0	0	0	0.0115(6)	0.938(3)
Ba2	24k	0.248(2)	0.5164(7)	0	0.0139(11)	¼
Ni1/Si1	6c	¼	0	½	0.0101(10)	0.231(5)/0.769(5)
Si2	16i	0.1850(1)	x	x	0.0103(7)	1
Si3	24k	0	0.3093(2)	0.1213(2)	0.0114(5)	1

Table S6: Atomic coordinates, displacement parameters (in Å^2) and site occupancies for $Ba_{7.90(2)}Ni_{1.60(4)}Si_{44.40(4)}$.

Atom	Site	x	y	z	U_{eq}	Occ.
Ba1	2a	0	0	0	0.0127(7)	0.951(3)
Ba2	24k	0.2533(9)	0.5168(3)	0	0.0175(14)	¼
Ni1/Si1	6c	¼	0	½	0.0123(11)	0.267(7)/0.733(7)
Si2	16i	0.1847(1)	x	x	0.0128(7)	1
Si3	24k	0	0.3098(2)	0.1219(2)	0.0137(6)	1